ACADEMIA ROMÂNĂ
Revue Roumaine de Chimie
https://www.icf.ro/rrch/

Rev. Roum. Chim.,
2024, *69*(3–4), 201–214
DOI: 10.33224/rrch.2024.69.3-4.10

SPECTRAL CHARACTERIZATION, ANTIBACTERIAL AND ANTIOXIDANT ACTIVITY OF 2-(5-BROMO-1*H*-BENZIMIDAZOL-2-YL)-(3'/4'/5'-SUBSTITUTED)PHENOLS AND SOME TRANSITION METAL COMPLEXES**

Aydin TAVMAN,[a*] Demet GÜRBÜZ,[b] Ayça Aktaş KARAÇELİK,[c] Dilşat Nigar ÇOLAK,[d] Derya EFE[c] and Adem ÇINARLI[b]

[a]Istanbul University – Cerrahpaşa, Faculty of Engineering, Department of Chemistry, Inorganic Chemistry Division, 34320, Avcilar, Istanbul, Turkey
[b]Istanbul University – Cerrahpaşa, Faculty of Engineering, Department of Chemistry, Organic Chemistry Division, 34320, Avcilar, Istanbul, Turkey
[c]Giresun University, Espiye Vocational School, 28600, Giresun, Turkey
[d]Giresun University, Dereli Vocational School, Department of Forestry, Giresun, 28950, Turkey

Received December 13, 2023

2-(5-Bromo-1*H*-benzimidazol-2-yl)-3'/4'/5'-substituted-phenols (**HL$_1$** – **HL$_{25}$**) were synthesized and characterized using various spectroscopic techniques. Then, Fe(III), Co(II), Ni(II), Cu(II), Zn(II), Ru(III) complexes of 2-(5-bromo-1*H*-benzimidazol-2-yl)phenol (**HL$_1$**) were prepared and the methods such as elemental analysis, thermogravimetric analysis (TGA), molar conductivity and magnetic moment measurements, FT-IR, fluorescence and NMR spectroscopy were used to make suggestions about structures of the complexes. It is interesting that the compounds **HL$_{12}$** and **HL$_{22}$** showed stronger fluorescence effects than the others. The common feature of these two compounds is that they have a fluorine substituent at the 4'-position on the phenol ring. In addition, antioxidant and antibacterial activity of the compounds were investigated. The first three compounds showing the best antioxidant activity are **HL$_{25}$** (trihydroxy derivative: 4-(5-bromo-1*H*-benzimidazol-2-yl)benzene-1,2,3-triol), **HL$_8$** (2,5-dihydroxy derivative) and **HL$_6$** (2,3-dihydroxy derivative). It was observed that **HL$_{25}$** showed higher antioxidant activity than the reference substances 3,5-di-*tert*-4-butylhydroxytoluene (BHT) and Trolox both in terms of 1,1-diphenyl-2-picrylhydrazyl radical (DPPH•) scavenging (0.0018 mg/mL) and ferric reducing / antioxidant power (FRAP) methods {trolox equivalent antioxidant capacity (TEAC) value: 1564.44±1.92}. The second and third hydroxy groups added to **HL$_1$** appear to significantly increase the antioxidant activity. It was determined that complexes of **HL$_1$** showed much better antioxidant effect with respect to **HL$_1$**. The derivatives with the highest antibacterial effect were found to be **HL$_{14}$** (nitro derivative), **HL$_8$**, **HL$_6$** and **HL$_{25}$** having moderate activity. The high levels of both antioxidant and antibacterial activities of **HL$_6$**, **HL$_8$** and **HL$_{25}$** indicate a correlation between their antibacterial and antioxidant effects. It was observed that the Ru(III) and Co(II) complexes showed moderate antibacterial activity whereas the ligand was inactive.

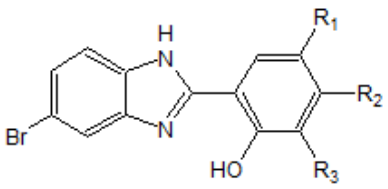

INTRODUCTION

Benzimidazole derivatives with hydroxyphenyl group attract the attention of researchers due to their interesting characteristics, and they are compounds that have application opportunities in many areas due to some of their properties. One of the most significant features of these compounds is

* Corresponding author: atavman@iuc.edu.tr
** Supplementary Information on https://www.icf.ro/rrch/ or https://revroum.lew.ro

that they are strong chelating compounds, *i.e.* ligands, by coordinating the phenolic oxygen and imidazole C=N nitrogen atoms to metal ion. In addition, many studies were published on the fluorescent characteristics of such compounds.[1–4]

Structural characteristics and antimicrobial activities of many benzimidazolylphenol derivatives and their various metal complexes were studied. For example, in the study examining the Ag(I), M(II) (M: Ru, Co, Ni, Pd, Cu, Cd, Hg) and Fe(III) complexes of 2-(5-nitro-1*H*-benzimidazol-2-yl)-4-bromophenol, it was found that some of the complexes showed significant activity against *S. aureus* and *C. albicans*.[5] Alterhoni *et al* reported that Co(II) complexes of 4-chloro-2-{5-(methyl/4,5-dimethyl/4-chloro-5-nitro)-1*H*-benzimidazol-2-yl} phenols have a wide range antimicrobial activity compared to the ligands and Pd(II), Cu(II) and Zn(II) complexes.[6] In the article that were studied 5-methoxy-2-(5-H/Me/F/Cl/Br/NO_2/OMe-1*H*-benzimidazol-2-yl)-phenols (**HL$_1$** – **HL$_7$**) and their complexes with $ZnCl_2$, it was observed that **HL$_4$**, $[Zn(\mathbf{HL_4})_2Cl_2]\cdot 2H_2O$, **HL$_5$**, **HL$_6$** and $[Zn(\mathbf{HL_6})_2Cl_2]\cdot 4H_2O$ exhibited antibacterial and antifungal activity against *S. aureus*, *E. faecalis* and *C. albicans*.[7] 2-(5-H/Me/F/Cl/NO_2-1*H*-benzimidazol-2-yl)-benzene-1,4-diols (**HL$_1$** – **HL$_5$**) and **HL$_1$** complexes with $Fe(NO_3)_3$ and $M(NO_3)_2$ (M: Co, Ni, Cu, Zn) were reported and found that all of the complexes have higher antifungal effect than the ligand. In addition Zn(II) complex was effective toward especially *S. aureus* and *S. epidermidis* (Gram-positive bacteria) that the ligand has lower effect on them.[8] 2-Methoxy-6-(5-H/Me/Cl/NO_2-1*H*-benzimidazol-2-yl)phenols (**HL$_1$** – **HL$_4$**) and **HL$_1$** complexes with $Fe(NO_3)_3$, $Cu(NO_3)_2$, $AgNO_3$ and $Zn(NO_3)_2$ were reported and it was observed that **HL$_1$** and **HL$_3$**, as well as the Cu(II) and Zn(II) complexes, showed antibacterial activity against Gram-positive bacteria.[9] Ru(III), Ni(II) and Cu(II) complexes of 2-(2-hydroxy phenyl)-1*H*-benzimidazole exhibited considerable activity against *Acinetobacter* and *P. aeruginosa* bacteria.[10] Our previous study, we synthesized and characterized 2-[4,6-{dichloro/dimethyl/bis-(trifluoromethyl)}-benzimidazol-2-yl]-(5-bromo/methoxy)-phenols and their complexes with $ZnCl_2$, $PdCl_2$ and $AuCl_3$.[11] We observed that the Au(III) complexes have superior activity against the bacteria, while the Pd(II) complexes showed higher antifungal activity than the ligands and the metal salt.

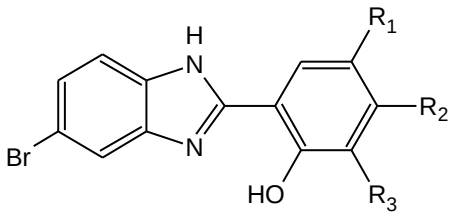

HL$_1$: R_1=R_2=R_3=H
HL$_2$: R_1=R_2=H, R_3=Cl
HL$_3$: R_1=Cl, R_2=R_3=H
HL$_4$: R_1=R_2=H, R_3=CH_3
HL$_5$: R_1=CH_3, R_2=R_3=H
HL$_6$: R_1=R_2=H, R_3=OH
HL$_7$: R_1=H, R_2=OH, R_3=H
HL$_8$: R_1=OH, R_2=R_3=H
HL$_9$: R_1=R_2=H, R_3=OCH_3
HL$_{10}$: R_1=H, R_2=OCH_3, R_3=H
HL$_{11}$: R_1=OCH_3, R_2=R_3=H
HL$_{12}$: R_1=F, R_2=R_3=H
HL$_{13}$: R_1=Br, R_2=R_3=H
HL$_{14}$: R_1=NO_2, R_2=R_3=H
HL$_{15}$: R_1=Cl, R_2=H, R_3=Cl
HL$_{16}$: R_1=Br, R_2=H, R_3=Br
HL$_{17}$: R_1=I, R_2=H, R_3=I
HL$_{18}$: R_1=Cl, R_2=H, R_3=OCH_3
HL$_{19}$: R_1=Br, R_2=H, R_3=OCH_3
HL$_{20}$: R_1=Br, R_2=H, R_3=F
HL$_{21}$: R_1=Cl, R_2=H, R_3=Br
HL$_{22}$: R_1=F, R_2=H, R_3=Cl
HL$_{23}$: R_1=Cl, R_2=H, R_3=I
HL$_{24}$: R_1=Br, R_2=OCH_3, R_3=Br
HL$_{25}$: R_1=H, R_2=R_3=OH

Fig. 1 – Structure of 2-(5-bromo-1*H*-benzimidazol-2-yl)-3'/4'/5'-substituted-phenols.

In this study, we synthesized and characterized 2-(5-bromo-1*H*-benzimidazol-2-yl)-phenol (**HL$_1$**) and its various derivatives (**HL$_2$** – **HL$_{25}$**, Fig. 1) and the complexes with Fe(III), Co(II), Ni(II), Cu(II), Zn(II), Ru(III) ions. In addition, fluorescence properties, antibacterial activities on two Gram-positive and two Gram-negative bacteria and antioxidant effects of the compounds were investigated. The substituent and complexation effects on the spectroscopic, antibacterial and antioxidant properties of the compounds were investigated. Some 2-(5-bromo-

1*H*-benzimidazol-2-yl)-3′/4′/5′-substituted phenols within the scope of our study were reported in literature: The antimicrobial activity of **HL$_{10}$** and its Zn(II) complex towards different microorganisms was investigated by our group.[7] It was reported that **HL$_{13}$** was obtained as an intermediate[12] and **HL$_1$**, **HL$_3$**, **HL$_5$** and **HL$_{13}$** were used as reagents in the synthesis of oxazepine derivatives.[13] α-Glucosidase and urease enzyme inhibitory effects of **HL$_1$**, **HL$_{10}$**, **HL$_{15}$** and **HL$_{21}$** were investigated.[14,15] The other compounds are obtained for the first time in this study.

RESULTS AND DISCUSSION

Some analytical data and physicochemical properties of the compounds are given in Experimental Section.

General Properties

In this study, twenty-five 2-(5-bromo-1*H*-benzimidazol-2-yl)-substituted-phenol derivatives (**HL$_1$** – **HL$_{25}$**) were synthesized and their physical and chemical properties were investigated and compared. Then, the complexes of **HL$_1$** with Fe(III), Co(II), Ni(II), Cu(II), Zn(II) and Ru(III) ions were prepared.

HL$_1$ is a bidentate, monodeprotonable and chelating ligand potentially. According to the elemental analysis data, the M:L ratio in the Zn(II) complex is 1:1, in the others 1:2 (bis-type). [Zn(**L$_1$**)Cl(H_2O)] was prepared in ethyl acetate whereas the other complexes were obtained in ethanol. Zn(II) ion, which did not form a complex in ethanol or methanol, was able to form a complex in ethyl acetate with **HL$_1$**. This is because Zn(II) is a weaker Lewis acid than the others.

It was determined that the Fe(III) complex with a molar conductivity value of 86.1 $\Omega^{-1}cm^2mol^{-1}$ shows 1:1 ionic character, and other complexes with a molar conductivity below 50 $\Omega^{-1}cm^2mol^{-1}$ are non-ionic according to Geary.[16]

According to analytical data such as elemental analysis and molar conductivity, the phenolic hydrogen atom was released along with the coordination of the phenolic oxygen atom in the complexes. The effective magnetic moment value (μ_{eff}) of [Fe(**L$_1$**)$_2$(Cl)(H_2O)], which is 5.19 BM at room temperature, is within the expected range for high spin Fe(III) complexes. This value was found to be 1.52 BM for the Cu(II) complex, [Cu(**L$_1$**)$_2$], and is close to the expected value of 1.73 BM for mononuclear Cu(II) complexes and is within acceptable limits. The room temperature μ_{eff} value of [Co(**L$_1$**)$_2$] (3.90 BM) is very close to the theoretical value (3.87 BM) for a d^7 metal ion with three unpaired electrons. This value can be associated with the fact that the Co(II) ion environment in the complex has a tetrahedral geometry. The low magnetic moment value of 1.98 BM of [Ni(**L$_1$**)$_2$], lower than the theoretical value of 2.83 BM for a d^8 ion (unpaired two electrons), may indicate a distorted structure between tetrahedral and square planar systems (quasi-tetrahedral).[17]

By reacting **HL$_1$** with Ru(II) under atmospheric conditions, a complex with paramagnetic character was obtained. This shows that Ru(II) is oxidized to Ru(III) having d^5 electronic configuration. The complexation reaction was carried out by passing air through the solution for complete oxidation with air oxygen. As a result, the magnetic moment value of the resulting complex was measured as 1.57 BM. It can be interpreted that the magnetic moment value of [Ru(**L$_1$**)$_2$(DMSO)$_2$Cl]·2H_2O corresponds to one unpaired electron for d^5 electronic configuration despite it is lower than the expected value (1.71 BM).[18]

Mass Spectra

ESI-MS results support formation of the benzimidazolylphenols (see supporting information). The mole peak of many compounds was determined as 100% abundance, and the mole peak of many compounds was determined as $[M+H]^+$ and $[M+2H]^+$. Only the mole peak of **HL$_{25}$** differed from the others by appearing as $[M-4H]^+$. No significant results were obtained from ESI-MS analysis for complex compounds (mole peaks of the complexes could not be detected).

FT-IR Spectra

In the IR spectra of most benzimidazolylphenols, a strong band is seen in the range of 3228 – 3386 cm^{-1} (See Experimental Section). This band is related to the combination of ν(O–H) and ν(N–H) frequencies and arises from the formation of intramolecular hydrogen bonding between C=N nitrogen and OH hydrogen atoms.[19–22] However, the NH and OH groups gave separate stretching vibration bands in the compounds **HL$_1$**, **HL$_6$**, **HL$_7$**, **HL$_8$**, **HL$_{13}$** and **HL$_{14}$** at the 3189 – 3482 cm^{-1} range. The 3333 cm^{-1} band of **HL$_1$** disappears upon complex formation. This indicates that the OH proton removed and the phenoxyl oxygen

atom coordinates to the metal ion (Fig. 2) except Ru(III) complex.[23]

The stretching and out-of-plane bending modes [ν(C–H) and δ(C–H)] of the aromatic rings are detected at the 3085 – 3055 cm^{-1} and 813 – 737 cm^{-1} wavenumber regions, respectively, for all the compounds. The stretching frequencies of the aromatic C=C and the imidazole C=N groups are expected to appear between 1673 and 1578 cm^{-1}. In the spectra of **HL_1**, the medium band at 1260 cm^{-1} can be assigned to ν(C–O) of the phenolic group and it shifted to the range of 1240 – 1250 cm^{-1} in the complexes as a result of the OH oxygen atom coordination. The bands of ν(C–O) were determined in the range of 1183 – 1286 cm^{-1} in the spectra of other benzimidazolylphenol derivatives (**HL_2** – **HL_{25}**).

The C–Br stretching vibrations are seen at the range of 547 – 595 cm^{-1} as medium bands in all of the compounds.[24] In iodine-containing compounds, **HL_{17}** and **HL_{23}**, the C–I vibrations bond can be detected around 550 cm^{-1}, in chlorine-containing compounds, the medium bands above 700 cm^{-1} (between 700 and 750 cm^{-1}) can be attributed to ν(C–Cl). The ν(C–F) is expected to give a band above 1000 cm^{-1} in derivatives containing fluorine; however it is not so easy to detect it due to interference with other bonds.[25]

The emergence of new bands of medium intensity around 530 cm^{-1} can be assigned to the ν(M–OC) vibration frequencies resulting due to OH oxygen atom coordination.[26] It was evaluated that the new bands appearing in the complexes between 421 – 433 cm^{-1} belong to the stretching vibration mode of the M–N bond formed as a result of the coordination of the C=N nitrogen atom.[27–29] The coordination of the C=N nitrogen atom can also be associated with the shift of the 1634 cm^{-1} band of the ligand to lower wavenumbers in the complexes spectra. The broad bands with medium characteristics between 3400 and 3300 cm^{-1} in the Fe(III), Zn(II) and Ru(III) complexes mightily support the presence of the H_2O molecules.

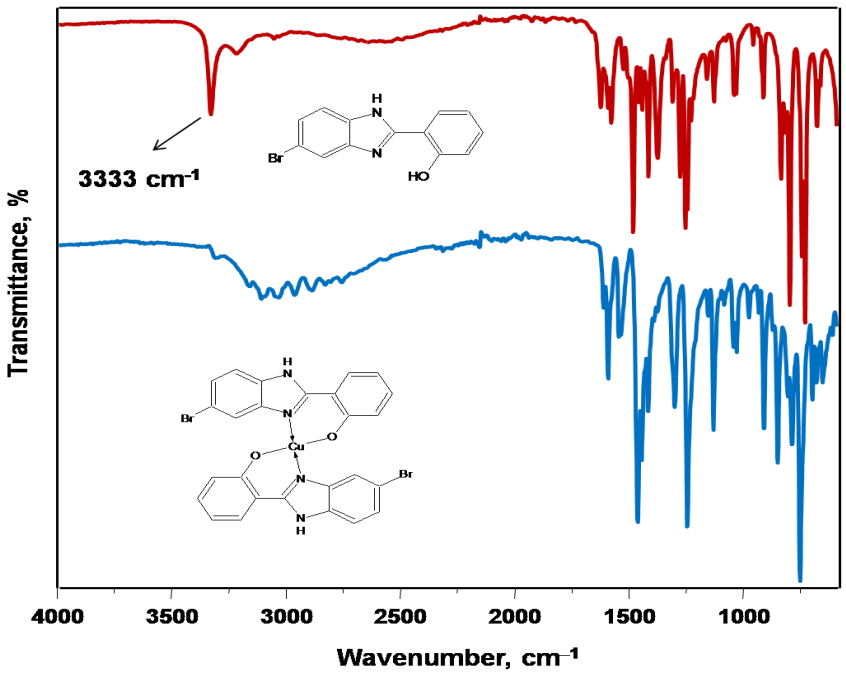

Fig. 2 – Comparison of the IR spectra of **HL_1** and its Cu(II) complex.

$Ru(DMSO)_4Cl_2$ (DMSO: dimethyl sulfoxide) was used to obtain the Ru(III) complex. According to the analysis results, it was determined that two moles of DMSO remained as coordinated in the complex. The bands belonging to DMSO in the complex were detected at 2920 cm^{-1}. DMSO coordinates to Ru(III) via the sulfur atom.[30]

According to the IR spectral data, **HL_2**, **HL_{15}**, **HL_{16}**, **HL_{17}**, **HL_{19}**, **HL_{20}**, **HL_{21}**, **HL_{22}**, **HL_{24}** and **HL_{25}** compounds also have keto form in the solid state (Fig. 3). In other words, there is a keto-enol mixture in these compounds. The weak or medium bands at 1718–1739 cm^{-1} range are considered to arise from the C=O bond in the keto form of the compounds in the solid state.

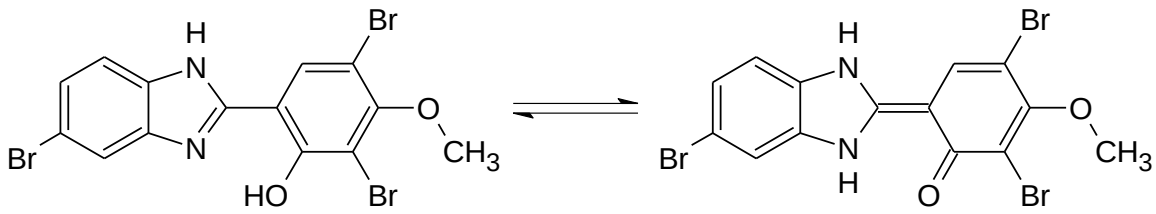

Fig. 3 – Keto-enol tautomer structures of **HL$_{24}$.**

NMR Spectra

^{1}H-NMR data of the benzimidazolylphenols (**HL$_1$** – **HL$_{25}$**) and the diamagnetic Zn(II) complex of **HL$_1$** with their assignments are given in Experimental Section. In the compounds **HL$_1$**, **HL$_2$**, **HL$_5$**, **HL$_6$**, **HL$_7$**, **HL$_8$**, **HL$_{13}$**, **HL$_{15}$**, **HL$_{16}$**, **HL$_{19}$** and **HL$_{22}$**, NH and OH protons give signals separately, while in the others both protons gave broad single signal only at the 14.00–11.21 ppm range. The reason why NH and H protons give single signals in most compounds is the formation of hydrogen bonds between C=N nitrogen and OH hydrogen atoms (Fig. 4a). In addition, according to NMR data, it is seen that there appear isomeric structures (A and B isomers) in **HL$_3$**, **HL$_5$**, **HL$_{13}$** and **HL$_{19}$** compounds. The isomeric structures of the aforementioned compounds are shown in Fig. 4. ^{1}H-NMR spectrum of the isomeric structure of **HL$_3$** is given in Fig. 5.

^{1}H-NMR spectra of **HL$_1$** and its Zn(II) complex are presented in Fig. 6. The absence of signal of the OH proton in the Zn(II) complex indicates that this proton was removed and the Zn–O covalent bond was formed.

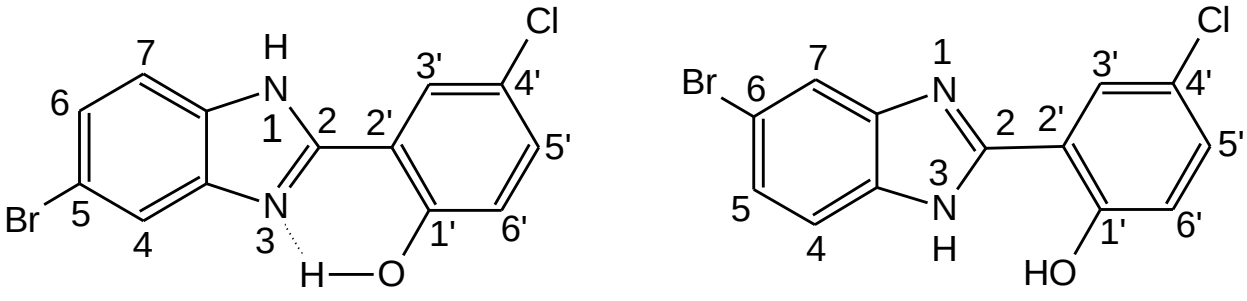

a b

Fig. 4 – Isomeric structures in 2-(5-bromo-1*H*-benzimidazol-2-yl)-4'-chlorophenol (**HL$_3$**).

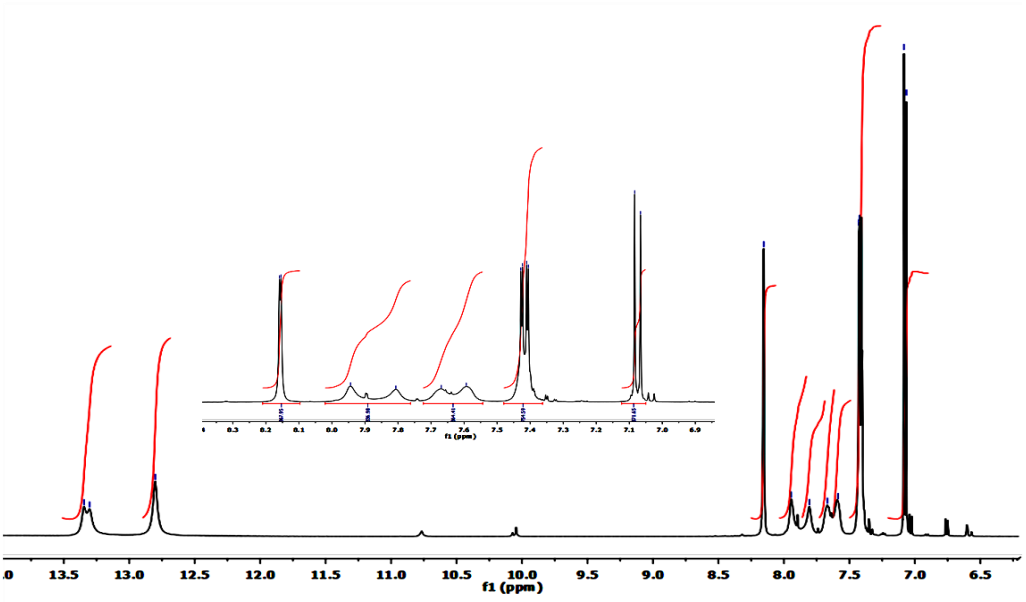

Fig. 5 – ^{1}H-NMR spectra of **HL$_3$** showing the isomeric structures.

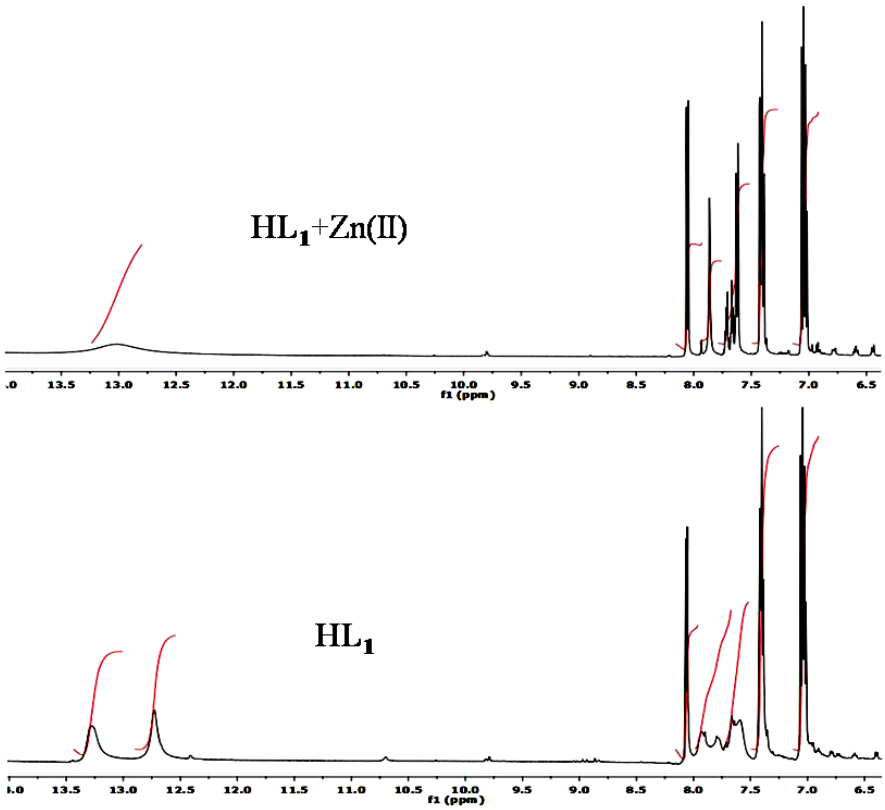

Fig. 6 – ^{1}H-NMR spectra of **HL$_1$** and its Zn(II) complex.

Fluorescence Spectra

Fluorescence spectral data of the compounds were obtained at a concentration of approximately 1×10^{-4} mol/L in ethanol at room temperature (excitation wavelength: 354 nm). The fluorescence spectral data of the compounds are given in Experimental Section. The fluorescence spectra of **HL$_1$** and some of its derivatives are given in Fig. 7, and the fluorescence spectra of the complexes are given in Fig. 8.

When the fluorescence spectra of the compounds are examined, it is seen that the highest blue shifted emission (lowest wavelength) belongs to the compounds **HL$_7$** (5'-hydroxy derivative: 442 nm) and **HL$_{10}$** (5'-methoxy derivative: 444 nm). The common feature of these two compounds is that they are 5'-substituted derivatives. **HL$_1$** ranks third among those emitting at the lowest wavelength, with a wavelength of 454 nm. The compounds with the longest wavelength (red shifted) emission are **HL$_8$** (4'-hydroxy derivative) with 511 nm, **HL$_{11}$** (4'-methoxy derivative) with 506 nm, and **HL$_6$** (6'-hydroxy derivative) with 490 nm.

The emission wavelength observed in the complexes is as follows: There is a significant decrease in the emission wavelengths of the Zn(II) and Co(II) complexes depending on the ligand (shifting to the left, blue shift from 454 nm to 416 nm), while almost no change was seen in the Ni(II) complex (λ_{max}: 452 nm). In others, a slight increase was detected between 460 and 465 nm (red shift). Fe(III) ion shows the highest quenching effect. While Co(II) shows the least quenching effect, Zn(II) ion comes in second. These two metal ions also show a blue shift effect. A relatively higher quenching effect was observed in the Cu(II), Ni(II) and Ru(III) complexes compared to the Co(II) and Zn(II) complexes.

Derivatives with the strongest fluorescence properties are **HL$_{12}$** (4'-fluoro derivative) and **HL$_{22}$** (6'-chloro-4'-fluoro derivative). The common point of these compounds is that both of them have a fluorine substituent at the 4' position. According to this observation, it can be concluded that the fluorine substituent increases the fluorescence intensity.

2-(2'-hydroxyphenyl)benzimidazole (HPBz) was examined by fluorescence spectroscopy and found that the most stable form of HPBz is the enol form in the ground state.[31–33] However, in the excited singlet state, where the OH group is much more acidic and the C=N nitrogen atom is much more basic than the ground state, the stable

structure has been reported to be the keto tautomer. This situation is explained by the excited-state intramolecular proton transfer (ESIPT) reaction. Similarly, in our study, it can be said that the keto form is more stable in the excited state (An example of keto-enol equilibrium is given in Fig. 3). The shifting towards shorter wavelength (redshift) observed in the complexes of **HL$_1$** can be considered as a result from the dominance of the enol form with the formation of the complex.

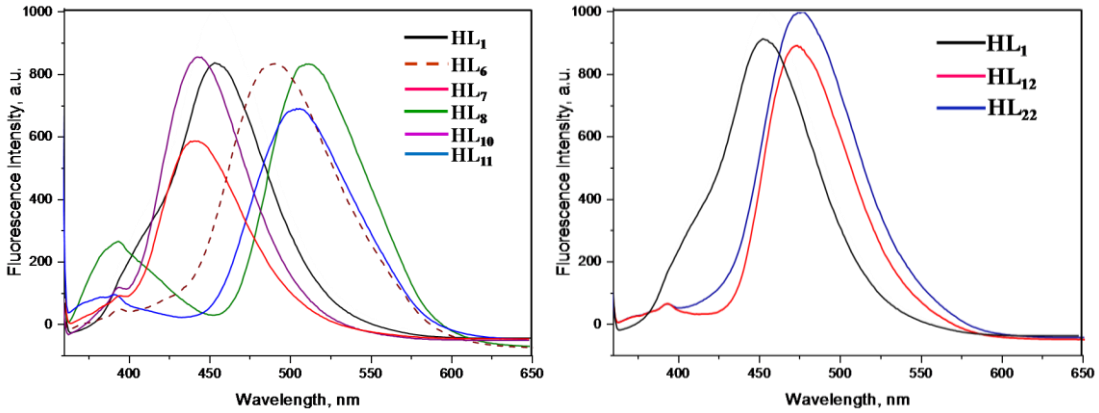

Fig. 7 – Comparing the fluorescence spectra of **HL$_1$** with **HL$_6$**, **HL$_7$**, **HL$_8$**, **HL$_{10}$** and **HL$_{11}$** (left), and with **HL$_{12}$** and **HL$_{22}$** (right).

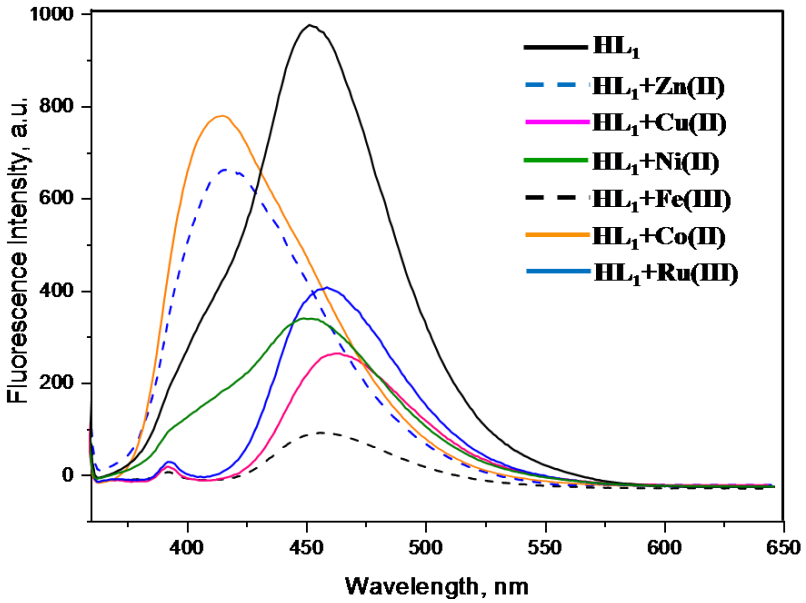

Fig. 8 – Fluorescence spectra of **HL$_1$** and its complexes.

Thermogravimetric Studies

Thermal analysis data of the complexes are outlined in the Experiment section. The thermal analysis curves of the **HL$_1$** complexes are represented in Fig. 9. The samples were heated from room temperature up to 800 ºC in air atmosphere. It is known that lattice water removed up to 100 °C and coordinate water up to 200 °C in thermal analysis. According to the thermal analysis data, lattice water is present in the Ru(III) complex only. In the Ru(III) complex, the ratio of one mole of water to mass is theoretically 1.95%, and the 2.1% mass loss seen in thermal analysis up to 100 °C can be considered as evidence for the presence of one mole of lattice water. In the Zn(II) complex, a mass loss of 4.5% is observed up to 150 °C, and a mass loss of 7.3% up to 200 °C. Considering the theoretical value of 4.4%, which corresponds to the ratio of one mole of H_2O to the mass of Zn(II) complex, it is possible to argue that the coordinated H_2O molecule removed around 150 °C. Considering the fact that one mole of H_2O in the Zn(II) complex corresponds to a

theoretical mass of 4.4%, it is possible to assert that the 4.5% mass loss around 150 °C corresponds to leaving of the coordinated H_2O molecule from the complex. Similarly, the coordinated water molecule in the Fe(III) complex is removed at around 150 °C. Again, in the Zn(II) complex, the 7.3% mass loss seen up to 200 °C can be interpreted that the chlorine atom starts leaving as HCl the complex around this temperature and completely remove up to 250 °C (totally 11.5% mass loss).

The TGA data shows that neither lattice nor coordinated H_2O molecules exist in the Co(II), Ni(II) and Cu(II) complexes. According to the TGA curves, metal oxide formation was observed in the Co(II), Ni(II) and Zn(II) complexes after 600 °C, while complete decomposition in the Ru(III) and Fe(III) complexes started earlier (just above 400 °C). The ratios of the masses remaining in the complexes after fully decomposition are in agreement with the theoretically calculated metal oxide mass ratios.

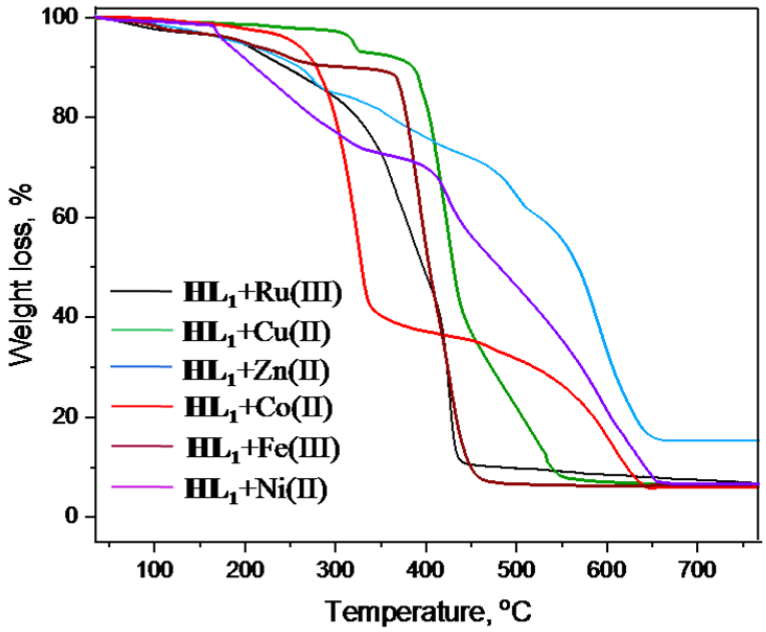

Fig. 9 – TGA curves of **HL_1** complexes.

Antioxidant Activity

In this study, the antioxidant activities of the compounds were tested by 1,1-diphenyl-2-picrylhydrazyl radical (DPPH•) scavenging activity and ferric reducing antioxidant power (FRAP) assays (Table 1). The higher the Trolox Equivalent Antioxidant Capacity (TEAC) values in the FRAP test and the lower the SC_{50} values in the DPPH• scavenging test, the better the antioxidant activity is considered.

Among the compounds tested, the best antioxidant activity was shown by **HL_{25}**, trihydroxy derivative. The DPPH• scavenging activity (SC_{50}) value of this compound is 0.0018 mg/mL, which is better than those of the reference substances (commercial standard) butylated hyrdoxytoluene (BHT, 0.0115±0.0001 mg/mL) and Trolox (6-hydroxy-2,5,7,8-tetramethylchroman-2-carboxylic acid, 0.0028 mg/mL). The other compounds with high antioxidant activity are **HL_8** (1',4'-dihydroxy derivative, 0.0029±0.0000), **HL_6** (1',6'-dihydroxy derivative, 0.0034±0.0000) and **HL_{14}** (4'-nitro derivative, 0.0092±0.0002). The structures of the first three compounds showing the best antioxidant activity are shown in Scheme 1. Except for **HL_{14}** (nitro derivative), these compounds have very high TEAC values ranging from 1473 to 1564 μM. The hydroxyl group added to **HL_1** appears to increase antioxidant activity. The SC_{50} values of the complexes were found at the range of 0.38 – 1.13 mg/mL and these values are considerably higher than the ligand (the antioxidant value of **HL_1** is 1.1485±0.0121 mg/mL). This result indicates that the metals bound to the ligand increase the antioxidant activity. In addition, the results of both antioxidant activity methods exhibited a good positive correlation (R^2: 0.8802).

Table 1

Antioxidant activities of the compounds and standards*

Compounds	DPPH• (SC_{50}, mg/mL)	FRAP (μM, TEAC)
HL_1	1.1485±0.0121	7.96±1.40
HL_2	0.5261±0.0099	60.74±0.85
HL_3	0.2740±0.0026	3.70±1.70
HL_4	0.0518±0.0006	954.81±0.64
HL_5	0.2678±0.0038	46.67±0.56
HL_6	**0.0034±0.0000**	**1472.96±1.79**
HL_7	0.1754±0.0003	196.85±3.70
HL_8	**0.0029±0.0000**	**1550.74±6.49**
HL_9	0.1442±0.0016	789.81±2.63
HL_{10}	0.4568±0.0136	20.56±2.42
HL_{11}	0.0414±0.0010	1044.81±3.35
HL_{12}	0.7989±0.0163	55.93±2.10
HL_{13}	0.0361±0.0039	78.52±1.79
HL_{14}	**0.0092±0.0002**	123.33±2.00
HL_{15}	0.2566±0.0026	74.81±3.53
HL_{16}	1.4074±0.0294	42.96±0.64
HL_{17}	0.2880±0.0055	44.26±1.70
HL_{18}	0.1335±0.0020	530.37±1.79
HL_{19}	0.2456±0.0000	483.33±3.09
HL_{20}	0.5850±0.0117	75.19±2.85
HL_{21}	-0.8491±0.0404	41.48±2.63
HL_{22}	0.3613±0.0011	33.52±0.85
HL_{23}	0.2535±0.0033	337.41±2.51
HL_{24}	1.0258±0.0174	63.52±2.80
HL_{25}	**0.0018±0.0000**	**1564.44±1.92**
HL_1+Fe(III)	0.4390±0.0020	69.81±0.85
HL_1+Co(II)	0.3779±0.0037	60.00±0.56
HL_1+Cu(II)	0.7314±0.0066	20.00±0.96
HL_1+Ni(II)	1.1254±0.0075	20.37±2.25
HL_1+Zn(II)	0.5131±0.0037	5.56±2.42
HL_1+Ru(III)	0.4822±0.0037	78.52±3.16
BHT	0.0115±0.0001	N.D.
Trolox	0.0028±0.0000	**

*: Each value represents the average of three repetitions. N.D.: not detected.
**: Trolox was used to create a calibration curve used for the calculation of TEAC values.

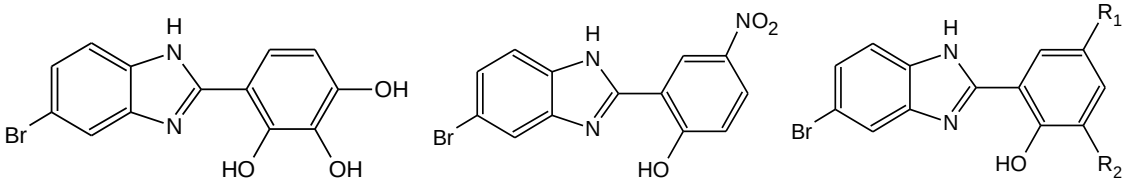

HL_{25} **HL_{14}** **HL_6**: R_1=H, R_2=OH
HL_8: R_1=OH, R_2=H

Scheme 1 – Chemical structures of the compounds with the highest DPPH• scavenging activity.

Antibacterial Activity

In vitro antibacterial activity of the compounds was tested against Gram-positive (*Bacillus subtilis* ATCC 6633 and *Enterococcus faecalis* ATCC 29212) and two Gram-negative (*Escherichia coli* ATCC25922 and *Salmonella typhimurium* ATCC14028) bacteria using disc diffusion method. Test results are shown in Table 2 in terms of minimum inhibitory concentration (MIC) values with together those of Ciprofloxacin for comparison. The derivatives with the highest antibacterial effect were found to be **HL_{14}** (nitro derivative, 125 μg/mL against to all tested bacteria), **HL_8**, **HL_6** and **HL_{25}**. MIC values of these compounds ranging from 125 to 250 μg/mL can be considered as moderate activity. Considering that

HL_6 is 3-hydroxy, **HL_8** is 5-hydroxy and **HL_{25}** is 3,4-dihydroxy derivatives, it can be concluded that additional OH groups attached to **HL_1** increase the antibacterial effect. The fact that the antioxidant activities of these compounds are also higher than the others indicates that there is a correlation between their antibacterial and antioxidant activities of them. Another noteworthy finding is that the antibacterial activity of **HL_1** is quite low (>700 μg/mL), against all the bacteria, whereas the Co(II) and Ru(III) complexes of it show moderate activity at 250–500 μg/mL.

Table 2

The minimal inhibition concentration (MIC) values of the compounds against the bacteria (μg/mL)

Compounds	Bacteria*			
	B.s.$^+$	*E.f.*$^+$	*E.c.*$^-$	*S.t.*$^-$
HL_1	–	–	–	–
HL_2	600	500	500	–
HL_3	600	700	–	700
HL_4	250	250	500	500
HL_5	700	–	–	–
HL_6	125	250	250	125
HL_7	250	250	500	500
HL_8	125	125	125	250
HL_9	600	700	600	600
HL_{10}	–	500	500	–
HL_{11}	250	250	500	500
HL_{12}	–	–	–	–
HL_{13}	600	700	–	–
HL_{14}	125	125	125	125
HL_{15}	600	500	–	500
HL_{16}	–	–	–	–
HL_{17}	700	500	500	500
HL_{18}	700	700	–	–
HL_{19}	600	–	–	600
HL_{20}	700	–	700	–
HL_{21}	700	600	–	500
HL_{22}	600	600	700	600
HL_{23}	–	–	–	700
HL_{24}	–	–	–	–
HL_{25}	125	250	250	250
HL_1+Fe(III)	–	–	–	–
HL_1+Co(II)	250	500	250	250
HL_1+Cu(II)	–	–	600	500
HL_1+Ni(II)	–	–	–	–
HL_1+Zn(II)	500	600	500	500
HL_1+Ru(III)	250	250	500	250
DMSO (100%)	–	\–	–	–
Ciprofloxacin	0.700	0.250	0.400	0.050

**B.s.*: *Bacillus subtilis* ATCC 6633, *E.f.*: *Enterococcus faecalis* ATCC 29212, *E.c.*: *Escherichia coli* ATCC25922, *S.t.*: *Salmonella typhimurium* ATCC14028.$^+$: Gram-positive,$^-$: Gram-negative. Ciprofloxacin: positive control, DMSO: Dimethyl sulfoxide, solvent and negative control.

EXPERIMENTAL

All chemicals and solvents were of reagent grade and they were used without further purification.

Analytical data were obtained with a Thermo Finnigan Flash EA 1112 analyzer. Melting points were determined using a Buchi M-560 melting-point apparatus. Molar conductivity of the complexes was measured on a WTW Cond315i conductivity meter in DMF at 25ºC. FT-IR spectra were recorded on a Bruker Optics Vertex 70 spectrometer using Attenuated Total Reflection (ATR) techniques between 400 and 4000 cm^{-1}. ^{1}H-NMR spectra were run on a Varian Unity Inova 500 NMR spectrometer. The residual DMSO-d_6 signal was also used as an internal reference. The Electron Spray Ionization-Mass Spectroscopy (ESI-MS) analyses were carried out in positive ion modes using a Thermo Finnigan LCQ Advantage MAX LC/MS/MS. Fluorescence spectra were performed on a Shimadzu RF-5301 PC Spectrofluorophotometer in EtOH ($c = 1\times10^{-4}$ mol/L). Magnetic moment measurements were carried out on MK1 Sherwood Scientific apparatus at room temperature by Gouy's method. $Hg[Co(SCN)_4]$ was used as a calibrant. Effective magnetic moments were calculated from the expression $\mu_{eff} = 2.828(\chi_M T)^{½}$, where χ_M is the molar magnetic susceptibility corrected for diamagnetism of the constituting atoms.

Synthesis of the 2-(5-Bromo-1H-benzimidazol-2-yl)-4'/5'/6'-substituted-phenols

The ligands were prepared according to the literature procedures.[34] For instance, 2-(5-bromo-1*H*-benzimidazol-2-yl)phenol (**HL₁**) were obtained by reaction of salicylaldehyde (0.244 g, 2 mmol) with an equivalent amount of $NaHSO_3$ (0.208 g, 2 mmol) at room temperature in ethanol+water mixture (20 mL + 5 mL) for ~3 h. The mixture was treated with 4-bromo-1,2-phenylenediamine (0.374 g, 2 mmol) in dimethylformamide (15 mL) and refluxed for approx. 3 h. The reaction mixture was then poured into water (500 mL); a precipitate was formed. The precipitate was filtered, dried and crystallized from ethanol. Some physicochemical and spectroscopic data for **HL₁** – **HL₂₅** are given in the supplementary file.

Preparation of the Complexes

[Fe(**L₁**)₂(Cl)(H_2O)]: 0.217 g **HL₁** (0.75 mmol) was dissolved in ethanol (10 mL) and 0.245 g of $FeCl_3·9H_2O$ (~0.75 mmol) was added to this solution. This mixture was refluxed for 3 h and then cooled to room temperature. The slightly turbid black solution was filtered and kept at room temperature. A precipitate was formed within about 5 days; it was then filtered and dried at room temperature. Black solid. Yield: 0.180 g (71%). Decomposition point (Dec. p.): >200 °C. Anal. calcd. for $C_{26}H_{18}Br_2ClN_4O_3Fe$ (%): C, 45.55; H, 2.65; N, 8.17; Found (%): C, 46.64; H, 2.99; N, 8.53. MW: 685.55 g/mol. μ_{eff} = 5.19 BM. Molar conductivity: 86.1 $\Omega^{-1}cm^2mol^{-1}$. FT-IR (ATR, cm^{-1}): 3274 m,br ν(H_2O), 3121 m,br ν(NH), 3065 w ν(CH_{arom}), 1618 m ν(C=N), 1600 m ν(C=C), 1560 m, 1474 m, 1308 m, 1240 m ν(C–O), 1218 m, 1135 m, 1040 m, 915 m, 856 m, 795 m, 743 s δ(CH_{arom}), 690 m, 667 m, 640 m, 589 m ν(C–Br), 569 m, 527 m ν(Fe–O), 464 m, 445 sh, 425 m ν(Fe–N). Fluorescence spectra (λ_{max}/nm): 461 m. TGA (temp., °C: weight loss, %): 50: 0.3; 75: 0.8; 100: 1.7; 150: 3.0 (H_2O); 200: 5.0; 250: 7.9; 300: 9.0; 350: 10.6; 400: 58.4; 450: 83.4; 500: 84; 550: 86.7; 600: 87.3; 650: 87.6; 700: 87.8; 750: 88.1; 800: 88.2 (Fe_2O_3%/2 = 11.7).

[Co(**L₁**)₂]: 0.217 g **HL₁** (0.75 mmol) was dissolved in methanol (10 mL) and 0.180 g of $CoCl_2·6H_2O$ (0.75 mmol) were added to the ligand solution. The dark red mixture was refluxed for 2 h and then cooled to room temperature. The slightly turbid solution was filtered and kept at room temperature. A precipitate was formed within about one week; it was then filtered and dried at room temperature. Tile red solid. Yield: 0.196 g (75%). Dec. p.: >200 °C. Anal. calcd. for $C_{26}H_{16}Br_2N_4O_2Co$ (%): C, 49.16; H, 2.54; N, 8.82; Found (%): C, 49.42; H, 2.69; N, 8.68. MW: 635.17 g/mol. μ_{eff} = 3.90 BM. Molar conductivity: 15.3 $\Omega^{-1}cm^2mol^{-1}$. FT-IR (ATR, cm^{-1}): 3212 m,br ν(NH), 3068 m ν(CH_{arom}), 2928 w, 1618 m ν(C=N), 1601 m ν(C=C), 1533 m, 1479 m, 1379 m, 1207 m, 1250 m ν(C–O), 1137 m, 1039 m, 919 m, 805 s δ(CH_{arom}), 746 s δ(CH_{arom}), 687 m, 590 m ν(C–Br), 561 m, 532 m ν(Co–O), 471 m, 429 m ν(Co–N). Fluorescence spectra (λ_{max}/nm): 460 s. TGA (temp., °C: weight loss, %): 50: 0.2; 75: 0.2; 100: 0.4; 150: 1.1; 200: 2.3; 250: 4.5; 300: 22.2; 350: 58.7; 400: 61.5; 450: 63.8; 500: 68.2; 550: 86.7; 600: 87.3; 650: 87.6; 700: 87.8; 750: 88.0; 800: 88.1 (Co_3O_4%/3.2: 11.8).

[Ni(**L₁**)₂]: 0.217 g **HL₁** (0.75 mmol) was dissolved in methanol (20 mL) and 0.178 g of $NiCl_2·6H_2O$ (0.75 mmol) were added to the ligand solution. The blackish mixture was refluxed for 2 h and kept at room temperature. After 2 days some precipitates were formed, filtered and dried at room temperature. Dark grey solid. Yield: 0.204 g (78%). Dec. p.: >150 °C. Anal. calcd. for $C_{28}H_{22}Br_2N_4O_3Ni$ (%): C, 49.18; H, 2.54; N, 8.82; Found (%): C, 50.03; H, 2.80; N, 8.58. MW: 634.93 g/mol. μ_{eff} = 1.98 BM. Molar conductivity: 45.6 $\Omega^{-1}cm^2mol^{-1}$. FT-IR (ATR, cm^{-1}): 3217 m,br ν(NH), 3073 m ν(CH_{arom}), 1628 m ν(C=N), 1600 m ν(C=C), 1487 m, 1420 m, 1246 m ν(C–O), 919 m, 839 m, 804 s δ(CH_{arom}), 743 s δ(CH_{arom}), 681 m, 590 m ν(C–Br), 534 m ν(Ni–O), 472 m, 452 w, 424 m ν(Ni–N). Fluorescence spectra (λ_{max}/nm): 403 sh, 452 s. TGA (temp., °C: weight loss, %): 50: 0.4; 75: 0.9; 100: 1.1; 150: 1.5; 200: 4.8; 250: 13.3; 300: 20.1; 350: 25.1; 400: 27.2; 450: 36.9; 500: 47.1; 550: 56.5; 600: 67.9; 650: 81.1; 700: 87.4; 750: 87.5; 800: 87.5 (NiO%: 11.8).

[Cu(**L₁**)₂]: 0.217 g **HL₁** (0.75 mmol) was dissolved in methanol (10 mL) and 0.181 g $Cu(NO_3)_2·3H_2O$ (0.75 mmol) in methanol (5 mL) was added to the ligand solution. A dark brown precipitate was formed immediately. After 2 h reflux, the precipitate was filtered, washed with methanol (5 mL) and dried at 70-80ºC. Dark brown solid. Yield: 0.212 g (80%). Dec. p.: >250 °C. Anal. calcd. for $C_{26}H_{16}Br_2N_4O_2Cu$ (%): C, 48.81; H, 2.52; N, 8.76; Found (%): C, 49.05; H, 2.38; N, 8.64. MW: 639.79 g/mol. μ_{eff} = 1.52 BM. Molar conductivity: 22.0 $\Omega^{-1}cm^2mol^{-1}$. FT-IR (ATR, cm^{-1}): 3117 m ν(NH), 3047 w ν(CH_{arom}), 1623 m ν(C=N), 1600 m ν(C=C), 1555 m, 1471 m, 1309 m, 1239 m ν(C–O), 1140 m, 1038 m, 919 m, 857 m, 760 s δ(CH_{arom}), 705 m, 662 m, 611 m, 593 m ν(C–Br), 539 m ν(Cu–O), 467 m, 420 m ν(Cu–N). Fluorescence spectra (λ_{max}/nm): 465 m,br. TGA (temp., °C: weight loss, %): 50: 0.2; 75: 0.3; 100: 0.7; 150: 1.0; 200: 1.4; 250: 2.1; 300: 4.1; 350: 8.2; 400: 40.7; 450: 71.4; 500: 86.9; 550: 86.7; 600: 87.3; 650: 87.6; 700: 87.8; 750: 88.0; 800: 88.0 (CuO%: 12.4).

[Zn(**L₁**)Cl(H_2O)]: 0.217 g **HL₁** (0.75 mmol) was dissolved in ethylacetate (10 mL) and 0.105 g of $ZnCl_2$ (0.75 mmol) was added to this solution. This mixture was refluxed for 3 h then the precipitate formed was filtered, washed with ethyl acetate (5 mL) and dried at room temperature. Light grey solid. Yield: 0.251 g (82%). Dec. p.: >200 °C. Anal. calcd. for $C_{13}H_{10}BrClN_2O_2Zn$ (%): C, 38.36; H, 2.48; N, 6.88; Found (%): C, 38.42; H, 2.62; N, 6.47. MW: 407.0 g/mol. Molar conductivity: 32.0 $\Omega^{-1}cm^2mol^{-1}$. FT-IR (ATR, cm^{-1}): 3260 m,br ν(H_2O+NH), 3067 w ν(CH_{arom}), 1619 m ν(C=N), 1596 m ν(C=C), 1557 m, 1486 m, 1435 m, 1300 m, 1241 m ν(C–O), 1146 m, 1047 m, 918 m, 808 m, 746 s δ(CH_{arom}), 695 m, 610 m, 595 m ν(C–Br), 566 m, 532 m ν(Zn–O), 509 m, 470 m, 433 m ν(Zn–N). ^{1}H-NMR (DMSO-d_6) δ_H, ppm: 13.02 s,br (1H, NH), 8.05 dd (1H, J=7.8, 1.5, H3'), 7.86 s (1H, H4), 7.62 d (1H, J=8.3, H7), 7.41 m (2H, H6+H5'), 7.05 d (1H, J=8.3, H6'), 7.02 t (1H, J=8.4, 8.2, H4'). Fluorescence spectra (λ_{max}/nm): 416 m. TGA (temp., °C: weight loss, %): 50: 0.3; 75: 1.9; 100: 2.7; 150: 4.5; 200: 7.3; 250: 11.5; 300: 19.1; 350: 23.2; 400: 29.7; 450: 34.7; 500: 44.1; 550: 55.0; 600: 78.7; 650: 79.8; 700: 81.2; 750: 81.5; 800: 81.6 (%ZnO: 20.0).

[Ru($\mathbf{L_1}$)$_2$(DMSO)$_2$Cl]·2H$_2$O: 0.217 g **HL$_1$** (0.75 mmol) was dissolved in methanol (10 mL) and 0.363 g of Ru(DMSO)$_4$Cl$_2$ (0.5 mmol) were added to the ligand solution. The black mixture was refluxed for 2 h and then filtered. In the filtrate, a black precipitate was formed after a week staying at room temperature. It was filtered and dried at room temperature. Black solid. Yield: 0.463 g (85%). Dec. p.: 150 °C. Anal. calcd. for $C_{30}H_{32}Br_2ClN_4O_6S_2Ru$ (%): C, 39.81; H, 3.56; N, 6.19; S, 7.09; Found (%): C, 37.76; H, 3.40; N, 6.89; S, 6.85. MW: 905.06 g/mol. μ_{eff} = 1.57 BM. Molar conductivity: 23.4 $\Omega^{-1}cm^2mol^{-1}$. FT-IR (ATR, cm^{-1}): 3173 m,br ν(H$_2$O+NH), 3055 m ν(CH$_{arom}$), 2920 m ν(CH$_{aliph}$), 1622 m ν(C=N), 1597 m ν(C=C), 1527 m, 1470 m, 1305 m, 1241 m ν(C–O), 1084 m, 1015 m, 918 m, 859 m, 818 m, 754 s δ(CH$_{arom}$), 692 m, 669 m, 638 m, 591 m ν(C–Br), 526 m ν(Ru–O), 472 m, 421 m ν(Ru–N). Fluorescence spectra (λ_{max}/nm): 461 m. TGA (temp., °C: weight loss, %): 50: 0.5; 75: 1.4; 100: 2.1; 150: 3.4; 200: 5.4; 250: 10.5; 300: 16.1; 350: 27.2; 400: 51.6; 450: 84.6; 500: 87.2; 550: 87.8; 600: 88.2; 650: 88.5; 700: 88.8; 750: 89.0; 800: 89.0 (Ru$_2$O$_3$%: 27.06/2 = 13.5).

Antibacterial Activity Determination

The samples were diluted with DMSO (pure) at 700, 600, 500, 250 and 125 µg/mL concentrations. The used microorganisms were two Gram-positive (*B. subtilis* ATCC 6633 and *E. faecalis* ATCC 29212) and two Gram-negative (*E. coli* ATCC 25922, and *S. typhimurium* ATCC 14028) bacteria. The antimicrobial activity procedure is the same as in our previous studies.[35,36] The method is given in detail in the supplementary file.

Antioxidant Activity Determination

1,1-Diphenyl-2-picrylhydrazyl (DPPH•) Radical Scavenging Activity

Radical scavenging activity of the compounds was tested with several modifications by using the commonly used DPPH• scavenging activity.[37] Each of the concentrations of the samples were mixed with 100 µM methanolic DPPH• solution in an equal volume (750 µL) and kept for 50 minutes at room temperature. Then, all experimental setups were spectrophotometrically measured at 517 nm. The concentrations corresponding to the absorbances found were plotted, and the 50% scavenging concentration (SC$_{50}$) values were calculated in mg/mL. Low SC$_{50}$ values indicated higher radical cleaning potential.

Ferric Reducing / Antioxidant Power (FRAP) Method

In this method, 50 µL of each tested samples was mixed with 1.5 mL of FRAP reagent and after 20 minutes the absorbance was spectrophotometrically measured at 595 nm. The absorbance of all tubes was compiled against pure water. The ferric reducing activity of each sample was determined by the calibration graph obtained using trolox in the range of 31.25 – 1000 µM and the micromolar trolox equivalent antioxidant capacity (TEAC) was determined.[38]

CONCLUSION

In the present study, a series of 2-(5-bromo-1*H*-benzimidazol-2-yl)phenol derivatives (**HL$_1$** – **HL$_{25}$**) synthesized and characterized. The complexes of **HL$_1$** with Fe(III), Co(II), Ni(II), Cu(II), Zn(II) and Ru(III) ions were prepared and some structural properties were investigated. It was found that the M:L ratio in the Zn(II) complex is 1:1, in the others 1:2 (bis-type) according to the analytical data. In addition, antioxidant activity of the compounds was studied using the free radical (DPPH•) scavenging and ferric reducing antioxidant power (FRAP) assays. The first three compounds showing the best antioxidant activity are trihydroxy, 2,5-dihydroxy and 2,3-dihydroxy derivatives: **HL$_{25}$**, **HL$_8$** and **HL$_6$**, respectively. It is observed that the antioxidant activity of compounds having second and third hydroxy groups increases significantly compared to **HL$_1$**. It is noteworthy that **HL$_{25}$** showed higher antioxidant activity than the reference substances BHT and trolox, both in terms of DPPH• scavenging (0.0018 mg/mL) and FRAP (TEAC value: 1564.44±1.92). On the other hand, the complexes of **HL$_1$** showed much better antioxidant effect with respect to **HL$_1$**.

Antibacterial activity of the compounds was studied by the disk diffusion method against *B. subtilis*, *E. faecalis* (Gram-positive), *E. coli* and *S. typhimurium* (Gram-negative) bacteria. The derivatives with the highest antibacterial effect were found to be **HL$_{14}$** (nitro derivative), **HL$_8$** (2,5-dihydroxy derivative), **HL$_6$** (2,3-dihydroxy derivative) and **HL$_{25}$** (trihydroxy derivative) having moderate activity, respectively. The fact that **HL$_6$**, **HL$_8$** and **HL$_{25}$** have high activity in terms of both antioxidant and antibacterial effects can be interpreted as a correlation between their antibacterial and antioxidant effects. Another important observation is that Co(II) and Ru(III) complexes of **HL$_1$** show moderate antibacterial effects, although the ligand itself is not active against bacteria. Fluorescence spectroscopy measurements showed that the derivatives with fluorine atom in the 4'-position (**HL$_{12}$** and **HL$_{22}$**) have more intense fluorescence characteristic than the others.

The proposed structures for the complexes in best accord with the experimental data are shown in Fig. 10.

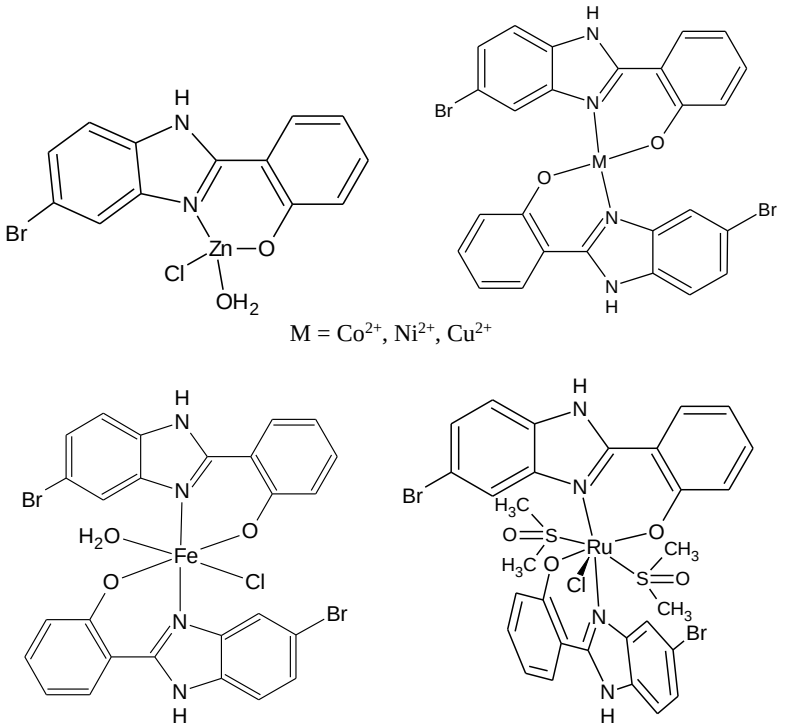

Fig. 10 – Suggested coordinations for the complexes.

Acknowledgments. This work was supported by Scientific Research Projects Coordination Unit of Istanbul University-Cerrahpasa. Project number: FYO-2017-24777

REFERENCES

1. R. Sathyanarayana, V. Kumar, G.H. Pujar, B. Poojary, M. K. Shankar and S. Yallappa, *J. Photochem. Photobiol. A: Chem.*, **2020**, *401*, Article ID 112751.
2. C. Li, D. Li, C. Ma and Y. Liu, *J. Mol. Liq.*, **2016**, *224*, 83–88.
3. N. Manojai, R. Daengngern, K. Kerdpol, C. Ngaojampa and N. Kungwan, *J. Lumin.*, **2017**, *188*, 275–282.
4. K. Akutsu, S. Mori, K. Shinmei, H. Iwase, Y. Nakano and Y. Fujii, *Talanta*, **2016**, *146*, 575–584.
5. A. Tavman, M. Hacioglu, D. Gürbüz, A. Cinarli, M.A.F. Oksüzömer and A. S. Birteksöz Tan, *Bull. Chem. Soc. Ethiop.*, **2019**, *33*, 451–466.
6. E. Alterhoni, A. Tavman, M. Hacioglu, O. Şahin and A. S. Birteksöz Tan, *J. Mol. Struct.*, **2021**, *1229*, Article ID 129498.
7. A. Tavman, D. Gürbüz, Ş. Öksüz and A. Cinarli, *Mor. J. Chem.*, **2018**, *6*, 328–341.
8. A. Tavman, A. Çınarlı, D. Gürbüz and A. S. Birteksöz, *J. Iran. Chem. Soc.*, **2012**, *9*, 815–825.
9. A. Tavman, S. Ikiz, A. F. Bagcigil, Y. N. Ozgür and S. Ak, *J. Serb. Chem. Soc.*, **2009**, *74*, 537–548.
10. Y. S. El-Sayed, M. Gaber and M. N. El-Nahass, *J. Mol. Struct.*, **2021**, *1229*, Article ID 129809.
11. A. Tavman, A. Z. Elmal, D. Gürbüz, M. Hacioglu, A. S. Birteksöz Tan and A. Cinarli, *Rev. Roum. Chim.*, **2023**, *68*, 49–59.
12. X. Chen, Y. Liao, Y. Liu, C. Zhu, T. Q. Chen and C. Zhong, *Dyes Pigm.*, **2017**, *139*, 420–430.
13. Y. Yin, Y.-Q. Zhang, B. Jin, S. Sha, X. Wu, C.B. Sangani, S.-F. Wang, F. Qiao, A.-M. Lu, P.-C. Lv and H.-L. Zhu, *Bioorg. Med. Chem.*, **2015**, *23*, 1231–1240.
14. T. Arshad, K. M. Khan, N. Rasool, U. Salar, S. Hussain, H. Asghar, M. Ashraf, A. Wadood, M. Riaz, S. Perveen, M. Taha and N. H. Ismail, *Bioorg. Chem.*, **2017**, *72*, 21–31.
15. T. Arshad, K. M. Khan, N. Rasool, U. Salar, S. Hussain, T. Tahir, M. Ashraf, A. Wadood, M. Riaz, S. Perveen, M. Taha, N. H. Ismail, *Med. Chem. Res.*, **2016**, *25*, 2058–2069.
16. W. Geary, *Coord. Chem. Rev.*, **1971**, *7*, 81–122.
17. A. G. Starikov, R. M. Minyaev and V. I. Minkin, *Chem. Phys. Lett.*, **2008**, *459*, 27–32. A. J. Bridgeman, *Dalton Trans.*, **2008**, *2008*, 1989–1992. D. Lomjansky, C. Rajnak, J. Titis, J. Monco, L. Smolko and R. Boca, *Inorg. Chim. Acta*, **2018**, *483*, 352–358.
18. A. M. Mansour, *Inorg. Chim. Acta*, **2013**, *394*, 436–445.
19. A. Tavman, N. M. Agh-Atabay, S. Güner, F. Gücin and B. Dülger, *Transit. Met. Chem.*, **2007**, *32*, 172–179.
20. A. Tavman, *Spectrochim. Acta A*, **2006**, *63*, 343–348.
21. D. Kanamori, Y. Yamada, A. Onoda, T. A. Okamura, S. Adachi, H. Yamamoto and N. Ueyama, *Inorg. Chim. Acta*, **2005**, *358*, 331–338.
22. N. Ueyama, N. Nishikawa, Y. Yamada, T. Okamura and A. Nakamura, *Inorg. Chim. Acta*, **1998**, *283*, 91–97.
23. V. M. Leovac, L. S. Jovanovic, V. S. Cesljevic, L. J. Bjwlica, V. B. Arion and N. V. Gerbelu, *Polyhedron*, **1994**, *13*, 3005–3014.
24. N. Sundaraganesan, C. Meganathan, B. Anand and C. Lapouge, *Spectrochim. Acta A*, **2007**, *66*, 773–780.
25. D. Mahadevan, S. Periandy, M. Karabacak and S. Ramalingam, *Spectrochim. Acta A*, **2011**, *82*, 481–492.
26. P. E. Kazin, M. A. Pogosova, L. A. Trusov, I. V. Kolesnik, O. V. Magdysyuk and R. E. Dinnebier, *J. Solid State Chem.*, **2016**, *237*, 349–357.
27. A. Tavman, S. Ikiz, A. F. Bagcigil, Y. N. Ozgür and S. Ak, *Turk. J. Chem.*, **2009**, *33*, 321–331.

28. K. Nakamoto, Infrared and Raman Spectra of Inorganic and Coordination Compounds, Part B, 5th edn., p. 26, John Wiley & Sons, Inc., New York, **1997**.
29. H. S. He, J. W. Huong and L. N. Ji, *Transit. Met. Chem.*, **1997**, *22*, 113–116.
30. B. N. Cunha, L. Colina-Vegas, A. M. Plutin, R. G. Silveira, J. Honorato, K. M. Oliveira, M. R. Cominetti, A. G. Ferreira, E. E. Castellano and A. A. Batista, *J. Inorg. Biochem.*, **2018**, *186*, 147–156.
31. X.-F. Yang, H. Qi, L. Wang, Z. Su and G. Wang, *Talanta*, **2009**, *80*, 92–97.
32. M. Mosquera, M. C. R. Rodriguez and F. Rodriguez-Prieto, *J. Phys. Chem. A*, **1997**, *101*, 2766–2772.
33. F. Rodriguez-Prieto, J. C. Penedo and M. Mosquera, *J. Chem. Soc. Faraday Trans.*, **1998**, *94*, 2775–2782.
34. H. F. Ridley, G. W. Spickett and G. M. Timmis, *J. Het. Chem.*, **1965**, *2*, 453–456; Z. Karimi-Jaberi and M. Amiri, *J. Chem.*, **2012**, *9*, Article ID 793978; O. S. Ürgüt, A. Tavman, M. G. Eser, *Chem. J. Mold.*, **2022**, *17*, 73–83.
35. A. A. Karaçelik, D. Efe, V. Çakir and Z. Bıyıklıoğlu, *JIST*, **2021**, *11*, 1302–1310.
36. Clinical and Laboratory Standards Institute (CLSI), Methods for dilution antimicrobial susceptibility tests for bacteria that grow aerobically, Approved Standard M7-A5, Wayne, PA, USA, **2006**.
37. S. A. Türkuçar, A. A. Karaçelik and M. Karaköse, *Turk. J. Chem.*, **2021**, *45*, 956–966.
38. A. A. Karaçelik, M. Küçük, Z. Iskefiyeli, S. Aydemir, S. De Smet, B. Miserez and P. Sandra, *Food Chem.*, **2015**, *175*, 106–114.